Quantum Chemical and RRKM Investigation of the Elementary Channels of the Reaction $C_6H_6 + O$ (^3P)

Devin Hodgson,[†] Hai-Yue Zhang, Mark R. Nimlos,[†,‡] and J. Thomas McKinnon[†]*

Department of Chemical Engineering, Colorado School of Mines, Golden, Colorado 80401, National Renewable Energy Laboratory, Golden, Colorado 80401

Received: November 9, 2000; In Final Form: February 5, 2001

We performed a computational study of an important reaction in the combustion of hydrocarbons, C_6H_6, + O (^3P), using ab initio and RRKM methods. Density functional theory (B3LYP) was used to optimize geometries and obtain molecular vibrational frequencies, and complete basis set extrapolation (CBS-QB3) was used to obtain the energies for the reactants several transition states and products. The initial formation of a stabilized adduct is characterized by a barrier of 4.9 kcal mol^{-1}, in good agreement with the measured activation energy for this reaction. All product channels originate from rearrangement or decomposition of this adduct, which our calculations suggest is a triplet ground state. All of our ab initio calculations are thus conducted on the triplet surface. There are several products that are energetically accessible at combustion temperatures, but the formation of phenoxy radical, C_6H_5O, and H atom dominate the product slate at low temperatures. Rearrangement to form formylcyclopentadiene, C_5H_5CHO, is also important at low temperatures, and the decomposition of this species to form cyclopentadienyl radical, C_5H_5, and HCO may be significant at higher temperatures. Rearrangement to form phenol is unimportant at all temperatures.

Introduction

The motivation for this work is to gain an understanding of one of the more important reactions involved in the high temperature oxidation of benzene. The combustion of aromatics in general, and benzene in particular, is important for several reasons. First, aromatic compounds are a large component of many of our fuels; for example, they comprise approximately 32% of gasoline.[1] Second, the pyrolysis of aromatic compounds is well-known to have high tendencies toward the production of soot and polycyclic aromatic hydrocarbons (PAH).[2] Finally, benzene and other aromatics are formed in flames of aliphatic fuel. A detailed understanding of the combustion mechanisms of benzene and other aromatics could help us design better processes to mitigate its adverse effects.

Interest in this study was prompted by an elementary reaction modeling study of low-pressure benzene combustion.[3] By employing the most commonly assumed product channel for the title reaction (i.e., $C_6H_5O + H$) and literature values for its rate constant, the concentration of phenoxy radical (C_6H_5O) is overpredicted by approximately 2 orders of magnitude. This problem with the phenoxy profile led to two possible hypotheses: (1) the production rate of phenoxy in our reaction mechanism is too high due to either incorrect rate constants or erroneous product channels or (2) the destruction rate of phenoxy in the mechanism is too low either due to errors in the literature rate constants or missing channels. The focus of this work is on the former hypothesis. That is, we report on our computer modeling investigation of the product channels for the reaction of benzene with triplet O atom and the rates for each channel.

The approach used in this work was ab initio quantum mechanical modeling of the reactants, unimolecular stabilized adducts, and transition states and subsequent RRKM modeling to determine rate constants. The results of our study provide insight into the mechanism for this important reaction.

The title reaction, $C_6H_6 + O$ (^3P), has a large number of energetically feasible product channels. Fortunately, many experimental studies have been carried out[4−13] with a few of the more pertinent results being summarized as follows. Nicovich et al.[6] measured absolute rate constants ($A = 2.8 \times 10^{13}$ cm^{3}mol^{-1} s^{-1}, $E_a = 4.9$ kcal mol^{-1}) for the reaction using flash photolysis-resonance fluorescence over a wide range of temperatures (298−950 K). This group found that their Arrhenius parameters were consistent with most of the previous measurements, which were made over a more narrow temperature span. Furthermore, the data were consistent with addition being the product channel, although the products were not directly measured. The most recent work by Ko et al.[7] using a method similar to Nicovich et al. over a temperature range of 600−1330 K returned Arrhenius parameters and conclusions very similar to those of ref 4. Benzene combustion modelers have employed the addition channel (product = phenol),[14,15] the abstraction channel (product = phenyl + OH),[14,15] and the addition/elimination channel (product = phenoxy + H).[3,16,17]

Reactions of ground-state O (^3P) with hydrocarbons have been extensively studied in the previous few decades. For alkanes, the only reported product channel is the abstraction of hydrogen leading to an alkyl radical and OH. The literature[18] on this type of reaction is largely in agreement, with *A*-factors near the gas kinetic limit ($>1.0 \times 10^{14}$ cm^{3}mol^{-1} s^{-1}) and activation energies of 6 to 10 kcal mol^{-1}, depending upon the strength of the C−H bond being broken. The picture becomes dramatically less clear when unsaturates are considered. In this case, the O atom can

* To whom correspondence should be addressed.
† Department of Chemical Engineering, Colorado School of Mines.
‡ National Renewable Energy Laboratory.

10.1021/jp004134a CCC: $20.00
Published on Web 04/04/2001

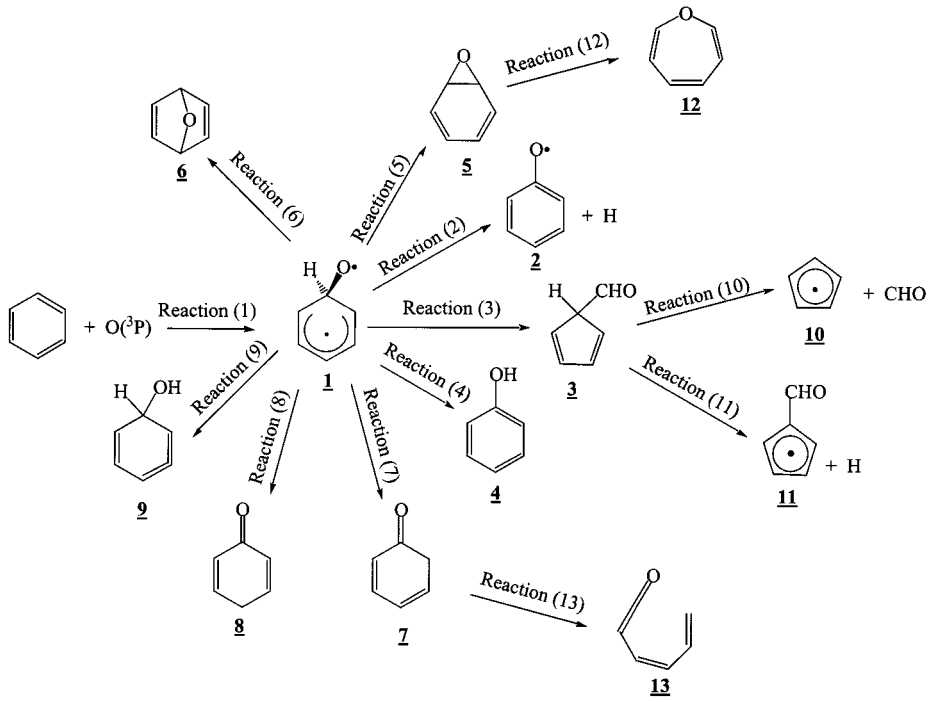

Figure 1. Reaction scheme considered for this study. All unimolecular product channels are formed in the triplet state.

still abstract hydrogen, but it can also undergo electrophillic addition to the molecule forming a triplet bi-radical followed by a number of possible chemically activated decomposition channels. For example, in the reaction O (^{3}P)+ C_2H_4 the following reaction product channels are reported: OH + C_2H_3, H + CH_2CHO, H_2 + CH_2CO, H + CH_3CO, CH_3 + HCO, CH_2 + CH_2O, and oxirane. Most O atom reactions involve free radical branching, which further underscores their importance in correctly modeling combustion chemistry.

Several studies involved the analysis of the title reaction using crossed molecular beams. One of the early studies[9] observed phenol, CO, and a polymeric material as products, but subsequent studies have found only a small amount of CO produced directly by this reaction. Probably the most detailed crossed molecular beeam investigation into possible reaction products was done by Sibener et al..[5] These authors observed an addition product (identified as phenol), a hydrogen elimination product (identified as phenoxy radical) and a small amount (<5%) of CO elimination. They also reached the conclusion that the energy barrier was in the range of 3−5 kcal mol^{-1}. Because the experiment involved nonthermal supersonic beams, this group did not compute Arrhenius parameters.

The most important result of the experimental studies with regard to our benzene modeling work is that they all appear to be in agreement on the rate of the reaction and that addition of O atom dominates over the abstraction channel. The final outcome of the adduct is not directly identified in any of the studies. The point of this study is to determine the product distribution from quantum chemical modeling, and to provide rate constants for these elementary reactions.

The reaction of ground state (^{3}P) atomic oxygen with benzene is most likely to proceed first by addition to the aromatic ring as in reaction 1 in Figure 1. Abstraction of a hydrogen to form OH and phenyl radicals is unlikely. Nicovitch et al.[6] found identical rate constants with deuterated benzene C_6D_6, leading to the conclusion that the reaction mainly occurs over the addition pathway. One can expect a small barrier for this reaction since the aromatic delocalization on the ring is broken. Similarly, a small barrier is found in the reaction of hydrogen atom to benzene.[19] One can easily estimate the heat of this reaction using known bond dissociation energies and estimates of resonance stabilization. The enthalpy of this reaction should be

$$\Delta H_{\text{react 1}} = D^\circ(\text{C=C} \rightarrow \text{C-C}) + \Delta_{\text{stab}}H(\text{benzene}) - D^\circ(\text{C-O}) - \Delta_{\text{stab}}H(\text{cyclohexadienyl})$$

where D°(C=C → C−C) is the dissociation energy of a π-bond in a double bond (58 kcal mol-1),[20] $\Delta_{\text{stab}}H$(benzene) is the aromatic stabilization energy of benzene (37 kcal mol^{-1}),[21] D°-(C−O) is a bond dissociation energy of a C−O bond (82 kcal mol^{-1})[22] and $\Delta_{\text{stab}}H$(cyclohexadienyl) is the stabilization energy of the 2,4-cyclohexadienyl radical (20 kcal mol-1).[23] Using these values, one obtains the value $\Delta H_{\text{react 1}} = -7$ kcal mol^{-1}. The unpaired electron on the oxygen atom is separated from the unpaired electron on the ring by a sp^3 carbon, and thus, one expects the ground state of **1** to be a triplet state. One would expect that the products formed from the reaction of atomic oxygen with benzene would arise from reactions of this chemically activated adduct. There are several possible energetically accessible exit channels that we considered for this study, shown in Figure 1.

Computational Approach

Our approach was to calculate the energies and vibrational frequencies of the molecules **1**−**13**, benzene, CO and HCO, the atoms H and O(^{3}P) and the transition states TS1-TS13 using electronic structure methods[24] and evaluate rate constants for reactions shown in Figure 1, using Rice Ramsperger Kassel Marcus (RRKM) reaction theory.[25] In this investigation, Gaussian 98[26] was used to calculate molecular properties and our own code was used for the RRKM calculations. Because the oxygen atom is a triplet in its ground state, we have conducted our ab initio calculations on the triplet surface. Our B3LYP and CBS-

TABLE 1: Arrhenius Fits of the Rate Constants for the Disappearance of Benzene and Oxygen, as Compared to Several Experimental Values

source	A (cm^3 mol^{-1} s^{-1})	E (kcal mol^{-1})
Tappe et al.[13]	2.1×10^{13}	4.4
Nicovitch et al.[6]	2.78×10^{13}	4.9
Ko et al.[7]	3.22×10^{13}	5.1
RRKM[a]	1.36×10^{14}	6.1

[a] This work, 100 Torr.

QB3 calculations suggest that the adduct **1** has a triplet ground state. All of the products, with the exception of the radical products, are singlets in their ground states. We did not attempt to calculate the intersystem crossing rates for hopping from the triplet surface to the singlet surface. The lifetimes of the intermediates in this study are very short at combustion temperatures (see below) compared to typical triplet lifetimes.[27]

Electronic Structure Calculations. Initially, geometries and energies were determined using MP4/6-31G(d)//HF/6-31G(d). However, this method of calculation proved time-consuming and inaccurate as is shown in Table 2 for reaction 1. Higher energy accuracy was obtained using the density functional technique, B3LYP,[28] and the correlation consistent basis set (cc-pVDZ) developed by Dunning.[29] The B3LYP technique has been shown to produce accurate energies at a low computational cost.[30] Furthermore, we have found that vibrational frequencies for stable compounds and radicals can be accurately determined using B3LYP.[31−35]

The results of our B3LYP calculations of the transition state for reaction 1, TS1, are gathered in Table 2. Though the results from the B3LYP method are an improvement over HF/6-31G-(d) and MP4/6-31G(d)//HF/6-31G(d), the transition state energy is still low relative to experiment. Earlier studies using the B3LYP technique have also demonstrated that experimental activation energies are often underestimated.[36−49] Consistent with this, our calculated barrier was 4−5 kcal mol^{-1} lower than the experimental value. This error did not improve with a larger basis set (cc-pVQZ). On the other hand calculations using B3LYP-optimized geometries and CCSD and QCISD energies are about 5 kcal mol^{-1} over experimental values. CBS-Q, which optimizes geometries with MP2, is also approximately 5 kcal mol^{-1} too high. To improve our energy calculations, we used a newly developed CBS extrapolation technique, CBS-QB3.[50] This technique obtains molecular geometries and vibrational frequencies using B3LYP. Using the improved geometries and vibrational frequencies of B3LYP relative to MP2, the CBS-QB3 technique has been shown to produce energies accurate to approximately 2.8 kcal mol^{-1}.[50] Our calculated energy barrier using CBS-QB3 is in excellent agreement with the experimental value as shown in Table 1.

The location of transition states in this study was determined using the Synchronous Transit Quasi Newton (STQN) method[51] available in Gaussian 98. In most cases, this technique was successful at locating a saddle point that appeared to connect the reactant(s) with the product(s). When this was unsuccessful, we would conduct a potential energy surface (PES) calculation, where the reaction coordinate was varied systematically and all other degrees of freedom were allow to relax. This technique provided a rough estimate of the geometry and energy of the transition state. The actual transition state could then be located easily using a Berny minimization. TS6, TS10, and TS11 were determined in this manner. There were some transition states where even this technique failed, and we could only get rough estimate of the transition state from the PES calculations. This was the case for reactions 8 and 9, which have large geometry changes in the transition state and high barriers. Thus, these channels do not contribute significantly.

RRKM Kinetics. From RRKM theory, the microcanonical rate constant is derived from the density of states of the unimolecular reactant and sum of states of the transition state. The microcanonical rate constant, in the notation of Holbrook,[52] is

$$k(E) = L^{\ddagger}\frac{Q^{\dagger}}{Q}\frac{W(E^{\dagger})}{h\rho(E)} \tag{1}$$

The impact of molecular properties on the RRKM theory can easily be seen in eq 1, where $L^{\ddagger}$ is the statistical reaction path degeneracy, Q is the partition function, $W(E)$ is the sum of states of the transition state, h is Planck's constant, and $\rho(E)$ is the density of states. The superscript "†" refers to the transition state properties. The sum of states is the integral of the density of states of the transition state structure from its zero point up to the energy of evaluation. The density of states of a molecule was calculated by assuming that all modes (vibrations, rotations, hindered rotations) are separable, and each vibration can be modeled as a harmonic oscillation. Each mode is convoluted together with the Stein-Rabinovitch[53] algorithm to get all the possible quantum energy levels of the molecule. RRKM theory is applicable to systems that adhere to the assumption of ergodicity; that is, the energy imparted in a collision is randomly distributed throughout all available modes of motion on the time scale of reaction.

As can be found in reference 52 the overall rate constant is determined by assuming a pseudo steady state on all energetically activated species, and integrating the resulting microcanonical expression over energy ranging from the barrier height to infinity (or a high enough energy that the Boltzmann distribution function annuls the contribution at that energy level).

For the formation of stabilized adduct, the rate constant is

$$k_{\mathrm{stab},\mathbf{1}} = K_{\mathrm{eq}}\int \frac{k_{-1}P(E)\mathrm{d}E}{1+\frac{k_{-1}}{\beta\omega}+\frac{k_2}{\beta\omega}+\frac{k_4}{\beta\omega}-\frac{\frac{k_3}{\beta\omega}\frac{k_{-3}}{\beta'\omega}}{1+\frac{k_{-3}}{\beta'\omega}+\frac{k_{10}}{\beta'\omega}+\frac{k_{11}}{\beta'\omega}}-\frac{\frac{k_5}{\beta\omega}\frac{k_{-5}}{\beta''\omega}}{1+\frac{k_{-5}}{\beta''\omega}}-\frac{\frac{k_{12}}{\beta''\omega}\frac{k_{-12}}{\beta'''\omega}}{1+\frac{k_{-12}}{\beta'''\omega}}-\frac{\frac{k_7}{\beta\omega}\frac{k_{-7}}{\beta''''\omega}}{1+\frac{k_{-7}}{\beta''''\omega}}} \tag{2}$$

where $P(E)$ is the Boltzmann distribution function divided by the partition function of all active modes in the adduct **1**. The collision factor β, evaluated below, is unique to each individual unimolecular stabilization channel. The equilibrium rate constant K_{eq} was calculated from statistical mechanics, via a ratio of the partition functions of benzene and oxygen reactants and product **1**, as shown in the equation

$$K_{\mathrm{eq}} = \frac{Q_{\mathrm{AB}}}{Q_{\mathrm{A}}Q_{\mathrm{B}}}\exp\left(\frac{-\Delta H}{k_{\mathrm{B}}T}\right) \tag{3}$$

Where the partition functions are calculated according to their ground-state energy, and ΔH is the change in enthalpy between the reactants (A and B) and product (AB).

TABLE 2: Comparison of Various Computational Methods for the Calculated Energy for Molecules in the Entrance Channel (Reaction 1)

method	energy in Hartrees (ZPE included) O (^{3}P)	C_6H_6	TS1	barrier height (kcal mol^{-1})
HF/6-31G(d)	−74.783 93	−230.70314	−305.486 94	−1.5
MP4/6-31G(d)//HF/6-31G(d)	−74.895 97	−231.58034	−306.455 47	11.5
B3LYP/cc-pVDZ	−75.068 49	−232.26296	−307.329 08	1.4
B3LYP/cc-pVQZ	−75.098 19	−232.34927	−307.446 73	0.4
QCISD-T/6-31G(d)//B3LYP/cc-pVDZ	−74.895 90	−231.49639	−306.373 17	11.9
QCISD(T)/6-31G(d)//B3LYP/cc-pVDZ	−74.896 68	−231.53150	−306.410 27	11.1
QCISD(T)/3-21G(d)/B3LYP/cc-pVDZ	−74.449 71	−230.00191	−304.427 69	14.9
B3LYP/6-311G(d,p)	−75.085 39	−232.30855	−307.391 77	1.1
CBS-QB3	−74.987 64	−231.88985	−306.869 11	4.9
experimental activation energy[6]				4.9

For formation of phenoxy radical, the resulting rate expression is

$$k_{\mathrm{e\,lim},\boldsymbol{2}} = K_{\mathrm{eq}} \int \frac{k_{-1}\dfrac{k_2}{\beta\omega}P(E)\mathrm{d}E}{1+\dfrac{k_{-1}}{\beta\omega}+\dfrac{k_2}{\beta\omega}+\dfrac{k_4}{\beta\omega}-\dfrac{\dfrac{k_3}{\beta\omega}\dfrac{k_{-3}}{\beta'\omega}}{1+\dfrac{k_{-3}}{\beta'\omega}+\dfrac{k_{10}}{\beta'\omega}+\dfrac{k_{11}}{\beta'\omega}}-\dfrac{\dfrac{k_5}{\beta\omega}\dfrac{k_{-5}}{\beta''\omega}}{1+\dfrac{k_{-5}}{\beta''\omega}}-\dfrac{\dfrac{k_{12}}{\beta''\omega}\dfrac{k_{-12}}{\beta'''\omega}}{1+\dfrac{k_{-12}}{\beta'''\omega}}-\dfrac{\dfrac{k_7}{\beta\omega}\dfrac{k_{-7}}{\beta''''\omega}}{1+\dfrac{k_{-7}}{\beta''''\omega}}} \tag{4}$$

The expression of the rate constant for the formation of stable formylcyclopentadiene is

$$k_{\mathrm{stab},\boldsymbol{3}} = K_{\mathrm{eq}} \int \frac{k_{-1}\dfrac{\dfrac{k_3}{\beta\omega}}{1+\dfrac{k_{-3}}{\beta'\omega}+\dfrac{k_{10}}{\beta'\omega}+\dfrac{k_{11}}{\beta'\omega}}P(E)\mathrm{d}E}{1+\dfrac{k_{-1}}{\beta\omega}+\dfrac{k_2}{\beta\omega}+\dfrac{k_4}{\beta\omega}-\dfrac{\dfrac{k_3}{\beta\omega}\dfrac{k_{-3}}{\beta'\omega}}{1+\dfrac{k_{-3}}{\beta'\omega}+\dfrac{k_{10}}{\beta'\omega}+\dfrac{k_{11}}{\beta'\omega}}-\dfrac{\dfrac{k_5}{\beta\omega}\dfrac{k_{-5}}{\beta''\omega}}{1+\dfrac{k_{-5}}{\beta''\omega}}-\dfrac{\dfrac{k_{12}}{\beta''\omega}\dfrac{k_{-12}}{\beta'''\omega}}{1+\dfrac{k_{-12}}{\beta'''\omega}}-\dfrac{\dfrac{k_7}{\beta\omega}\dfrac{k_{-7}}{\beta''''\omega}}{1+\dfrac{k_{-7}}{\beta''''\omega}}} \tag{5}$$

The formation of the cyclopentyl radical and the formyl radical is

$$k_{\mathrm{e\,lim},\boldsymbol{10}} = K_{\mathrm{eq}} \int \frac{k_{-1}\dfrac{\dfrac{k_3}{\beta\omega}\dfrac{k_{10}}{\beta'\omega}}{1+\dfrac{k_{-3}}{\beta'\omega}+\dfrac{k_{10}}{\beta'\omega}+\dfrac{k_{11}}{\beta'\omega}}P(E)\mathrm{d}E}{1+\dfrac{k_{-1}}{\beta\omega}+\dfrac{k_2}{\beta\omega}+\dfrac{k_4}{\beta\omega}-\dfrac{\dfrac{k_3}{\beta\omega}\dfrac{k_{-3}}{\beta'\omega}}{1+\dfrac{k_{-3}}{\beta'\omega}+\dfrac{k_{10}}{\beta'\omega}+\dfrac{k_{11}}{\beta'\omega}}-\dfrac{\dfrac{k_5}{\beta\omega}\dfrac{k_{-5}}{\beta''\omega}}{1+\dfrac{k_{-5}}{\beta''\omega}}-\dfrac{\dfrac{k_{12}}{\beta''\omega}\dfrac{k_{-12}}{\beta'''\omega}}{1+\dfrac{k_{-12}}{\beta'''\omega}}-\dfrac{\dfrac{k_7}{\beta\omega}\dfrac{k_{-7}}{\beta''''\omega}}{1+\dfrac{k_{-7}}{\beta''''\omega}}} \tag{6}$$

The rates of other channels are computed using a similar logic.

Factors for the reactions 6, 8, 9, and 13 were not considered because the zero point energy of the transition states were high, and consequently, the contributions of these reactions would be expected to be negligible.

To account for collisional stability, we follow a method utilizing Gilbert's[54] modification to the collision factor, which is a correction to the strong collision theory in which every collision completely deactivates a molecule. We also used an empirical collision integral found in Gilbert and Smith[55] which describes the frequency of collisions based loosely on kinetic theory. The collision factor, β, is calculated from an approximation of all the collisions that will activate or deactivate an excited single molecule. The equation for the collision factor follows.

$$\beta \approx \frac{\left(\dfrac{\langle E_{\mathrm{down}}\rangle}{\langle E_{\mathrm{down}}\rangle + \mathrm{F_e}k_{\mathrm{b}}T}\right)^2}{\displaystyle\int_0^{E_{\mathrm{o}}} \rho(E)e^{-}E/k^{\mathrm{b}}T\left(1-\frac{F_{\mathrm{e}}}{1-F_{\mathrm{e}}}e^{\,\mathrm{E_o}-E/F^{\mathrm{e}}}\right)\mathrm{d}E} \tag{7}$$

$$F_{\mathrm{e}} = \frac{\displaystyle\int_{E_{\mathrm{o}}}^{\infty}\rho(E)e^{\,-E/k^{\mathrm{b}}T}\,\mathrm{d}E}{\rho(E_{\mathrm{o}})e^{\,-E/k_{\mathrm{b}}T}\,k_{\mathrm{b}}T} \tag{8}$$

Wang[56] verifies this formulation of the weak collision factor. The average downward energy per collision $\langle E_{\mathrm{down}}\rangle$ quantity is taken from a small collection compiled by Wang. The code used to calculate the kinetic rate constants uses the method of Wang, except for some minor additions. These additions include a quantum evaluation of the density of states of hindered internal rotation.

There was only one internal rotation in the mechanism, occurring on the formylcyclopentadiene ***3*** species, but the barrier to rotation was small (as estimated from the vibrational frequency and internal moment of inertia) enough that approximating the mode as a free rotation did not alter the results.

Results

As discussed above, RRKM calculations require the energies of reactants and transition states as well as vibrational frequencies and rotational constants. (There are no hindered rotors of importance in this study.) We have collected the values needed for RRKM calculations in Table 3, which shows the calculated energies, including zero point energies, of the product channels and transition states calculated using CBS-QB3. In addition to the absolute energies at 0 K, Table 3 shows the energies (in kcal mol^{-1}) for all species relative to the reactants: C_6H_6 + O (^{3}P). Vibrational frequencies and rotational constants are also reported in Table 3, and the imaginary frequencies of the transition states are indicated by a succeeding *i*. These molecular parameters are determined at the B3LYP/6−311 g(d,p) level. Figure 2 shows the atom numbering scheme for this study, and Table 4 shows some of the important bond lengths for the transition states, whereas Figure 3 shows the molecular structures of the calculated transitions states.

Figure 4 shows the computed surface for the reactions of the C_6H_6 + O adduct on the triplet surface. The first step of the reaction is the addition of O (^{3}P) to benzene, which is exothermic

TABLE 3: Vibration Frequencies,Energies, and Rotational Constants Calculated with CBS-QB3

species	energy[a](hartree)	ΔE^b_{rel} (kcal mol^{-1})	ν^cunscaled, A, B, C (cm^{-1},GHz)
	reaction 1 $C_6H_6 + O(^3P) \rightarrow TS1 \rightarrow C_6H_6O$		
C_6H_6 ($\tilde{X}$, $^1A_{1g}$)	−231.790 69		412, 412, 623, 623, 687, 723, 861, 861, 980, 980, 1013, 1015, 1023, 1060, 1060, 1175, 1198, 1198, 1335, 1382, 1513, 1513, 1637, 1637, 3156, 3165, 3165, 3181, 3181, 3192 *A*, *B*, *C* = 5.709 13, 5.709 13, 2.854 57
O (^{3}P)	−74.987 64		
$C_6H_6 + O(^3P)$	−306.778 33	0.0	
TS1 ($\tilde{X}$, $^3A''$)	−306.770 45	4.9	480i, 127, 186, 368, 406, 592, 605, 655, 710, 822, 887, 958, 964, 990, 1010, 1030, 1038, 1052, 1142, 1178, 1194, 1257, 1380, 1481, 1501, 1572, 1599, 3165, 3172, 3181, 3191, 3192, 3202 *A*, *B*, *C* = 4.223 69, 2.843 66, 2.121 96
1, C_6H_6O ($\tilde{X}$, $^3A''$)	−306.792 28	−8.8	64, 281, 387, 432, 515, 591, 614, 686, 753, 796, 844, 943, 970, 975, 990, 1000, 1053, 1125, 1175, 1194, 1311, 1369, 1408, 1429, 1431, 1539, 1579, 2683, 3159, 3162, 3186, 3188, 3197 *A*, *B*, *C* = 4.983 88, 2.734 42, 1.870 02
	reaction 2 $C_6H_6O \rightarrow TS2 \rightarrow C_6H_5O$ (phenoxy) + H		
TS2 ($\tilde{X}$, $^3A''$)	−306.783 80	−3.4	1014i, 170, 358, 430, 486, 516, 555, 594, 650, 714, 767, 796, 846, 946, 979, 982, 992, 1004, 1086, 1159, 1165, 1261, 1330, 1340, 1429, 1454, 1540, 1586, 3166, 3181, 3191, 3198, 3201 *A*, *B*, *C* = 5.289 95, 2.694 05, 1.831 68
2, C_6H_5O ($\tilde{X}$, $^2B_1$)	−306.302 59		191, 380, 446, 484, 531, 598, 656, 802, 804, 805, 928, 984, 988, 1000, 1009, 1089, 1163, 1165, 1272, 1337, 1419, 1443, 1480, 1546, 1587, 3166, 3172, 3188, 3195, 3198 *A*, *B*, *C* = 5.525 15, 2.789 13, 1.853 48
H	−0.499 82		
$C_6H_5O + H$	−306.802 41	−15.1	
	reaction 3 $C_6H_6O \rightarrow TS3 \rightarrow C_5H_5CHO$ (formylcyclopentadiene)		
TS3 ($^3A'$)	−306.781 18	−1.8	392i, 170, 206, 412, 487, 554, 683, 689, 725, 748, 794, 827, 907, 932, 946, 978, 1042, 1056, 1083, 1118, 1275, 1291, 1339, 1344, 1377, 1409, 1478, 3009, 3116, 3200, 3205, 3227, 3238 *A*, *B*, *C* = 4.64223, 2.85765, 2.76106
3, C_5H_5CHO (ã, $^3A'$)	−306.798 54	−12.7	56, 131, 219, 293, 410, 423, 540, 678, 713, 717, 812, 829, 853, 915, 968, 988, 1028, 1059, 1121, 1228, 1266, 1278, 1336, 1366, 1405, 1562, 1806, 2848, 2896, 3204, 3214, 3225, 3235 *A*, *B*, *C* = 5.464 94, 2.252 40, 1.940 43
	reaction 4 $C_6H_6O \rightarrow TS4 \rightarrow C_6H_5OH$ (phenol)		
TS4 ($^3A'$)	−306.753 96	15.3	2040i, 121, 295, 377, 428, 524, 534, 578, 597, 699, 717, 792, 820, 962, 965, 966, 977 ,1038, 1078, 1094, 1187, 1232, 1333, 1379, 1428, 1537, 1594, 2258, 3159, 3161, 3189, 3190 ,3198 *A*, *B*, *C* = 4.895 83, 2.745 62, 1.876 63
4, C_6H_5OH (ã, $^3A'$)	−306.804 86	−16.6	88, 173, 254, 392, 408, 522, 526, 530, 557, 558, 639, 669, 819, 917, 978 ,994, 1002, 1151, 1191, 1240, 1321, 1345, 1419, 1448, 1552, 1577, 2909, 3151, 3190, 3216, 3225, 3260, 3772 *A*, *B*, *C* = 5.305 82, 2.672 67, 1.777 37
	reaction 5 $C_6H_6O \rightarrow TS5 \rightarrow C_6H_6O$ (benzene oxide)		
TS5 ($^3A'$)	−306.778 02	0.2	557i, 176, 300, 378, 441, 544, 577, 627, 663, 757, 819, 880, 943, 951, 963, 982, 1034, 1072, 1147, 1185, 1232, 1349, 1382, 1403, 1418, 1456, 1591, 3050, 3165, 3181, 3185, 3197, 3213 *A*, *B*, *C* = 4.605 61, 3.330 72, 2.231 82
5, benzene oxide (ã, $^3A'$)	−306.781 04	−1.7	150, 246, 371, 385, 536, 542, 576, 610, 625, 744, 770, 849, 926, 948, 975, 997, 1017, 1075, 1138, 1190, 1248, 1344, 1378, 1403, 1407, 1438, 1625, 3119, 3127, 3166, 3180, 3189, 3196 *A*, *B*, *C* = 4.684 66, 3.358 20, 2.220 68
	reaction 6 $C_6H_6O \rightarrow TS6 \rightarrow C_6H_6O$ (bicyclo[2,2,1]hepta-7-oxa-2,5−diene)		
TS6	−307.282 56	25.4	492i, 305, 415, 492, 596, 649, 689, 703, 755, 761, 809, 869, 953, 984, 992, 1015, 1033, 1036, 1050, 1052, 1064, 1261, 1275, 1289, 1307, 1381, 1392, 3187, 3219, 3224, 3234, 3239, 3251 *A*, *B*, *C* = 4.110 99, 3.773 23, 3.752 60
6, bicyclo[2,2,1]hepta-7-oxa-2,5-diene (ã, $^3A_2$)	−306.756 84	13.5	145, 388, 420, 444, 533, 546, 587, 661, 739, 755, 813, 827, 895, 899, 918, 948, 1008, 1022, 1096, 1108, 1197, 1222, 1245, 1280, 1319, 1319, 1443, 3163, 3167, 3233, 3233, 3239, 3252 *A*, *B*, *C* = 4.065 95, 4.042 00, 3.702 86
	reaction 7 $C_6H_6O \rightarrow TS7 \rightarrow C_6H_6O$ (2,4−cyclohexadienone)		
TS7 ($^3A'$)	−306.778 02	19.2	1868i, 180, 244, 422, 439, 511, 566, 572, 685, 749, 809, 830, 872, 952, 960, 982, 1046, 1112, 1151, 1168, 1224, 1283, 1357, 1397, 1436, 1469, 1518, 1654, 2985, 3155, 3178, 3186, 3204 *A*, *B*, *C* = 5.069 59, 2.854 88, 1.887 28

TABLE 3 (Continued)

species	energy[a](hartree)	ΔE^b_{rel} (kcal mol^{-1})	ν^cunscaled, A, B, C (cm^{-1},GHz)
	reaction 7 $C_6H_6O \rightarrow$ TS7 $\rightarrow C_6H_6O$ (2,4−cyclohexadienone)		
7, 2,4-cyclohexadienone (ã, ^{3}A′)	−306.829 58	−32.2	35, 182, 421, 440, 468, 498, 552, 576, 695, 755, 805, 887, 915, 951, 961, 993, 1101, 1166, 1166, 1261, 1332, 1389, 1406, 1429, 1442, 1511, 1594, 2963, 2966, 3163, 3178, 3188, 3201 *A*, *B*, *C* = 5.191 17, 2.641 89, 1.769 44
	reaction 8 $C_6H_6O \rightarrow$ TS8 $\rightarrow C_6H_6O$ (2,5−cyclohexadienone)		
TS8[d]	−307.26311 [B3LYP]	[45.5]	
8, 2,5-cyclohexadienone (ã, ^{3}A″)	−306.802 30	−15.0	103, 268, 347, 391, 483, 505, 600, 656, 694, 775, 880, 917, 921, 950, 958, 966, 1117, 1183, 1188, 1193, 1267, 1340, 1393, 1411, 1456, 1513, 1598, 2898, 2917, 3164, 3164, 3192, 3193 *A*, *B*, *C* = 5.322 90, 2.613 25, 1.771 36
	reaction 9 $C_6H_6O \rightarrow$ TS9 $\rightarrow C_6H_6O$ (2,4,5−cyclohexatrienol)		
TS9[d]	−307.235 46 [B3LYP]	[62.8]	
9, 2,4,5-cyclohexatrienol (ã, ^{3}A′)	−306.787 95	−6.0	103, 197, 311, 417, 435, 522, 571, 591, 705, 763, 789, 859, 927, 957, 1001, 1013, 1021, 1089, 1170, 1202, 1250, 1294, 1332, 1388, 1416, 1499, 1585, 2884, 3148, 3167, 3173, 3193, 3813 *A*, *B*, *C* = 5.226 59, 2.650 05, 1.888 16
	reaction 10 $C_5H_5CHO \rightarrow$ TS10 $\rightarrow C_5H_5 + CHO$		
TS10 (^{3}A′)	−306.775 67	1.7	465i, 86, 120, 214, 313, 476, 494, 654, 693, 743, 753, 769, 837, 910, 925, 938, 988, 1037, 1058, 1128, 1176, 1258, 1294, 1379, 1413, 1536, 1794, 2710, 3191, 3211, 3218, 3223, 3240 *A*, *B*, *C* = 4.506 04, 2.327 15, 2.185 87
10, C_5H_5 ($\tilde{X}$, $^2B_1$)	−193.084 27		18, 501, 516, 584, 722, 821, 837, 893, 901, 918, 943, 1053, 1063, 1138, 1203, 1278, 1381, 1500, 1536, 3205, 3211, 3223, 3241, 3249 *A*, *B*, *C* = 9.225 79, 8.455 24, 4.411 86
HCO ($\tilde{X}$, ^{2}A′)	−113.704 74		1111,1942,2618 *A*, *B*, *C* = 706.82398, 44.97519, 42.28462
$C_5H_5 + CHO$	−306.789 01	−6.7	
	reaction 11 $C_5H_5CHO \rightarrow$ TS11 $\rightarrow C_5H_4CHO + H$		
TS11 (^{3}A′)	−306.763 21	9.5	566i, 159, 194, 271, 348, 435, 473, 509, 538, 714, 728, 782, 806, 834, 926, 946, 949, 1018, 1041, 1126, 1204, 1253, 1275, 1371, 1418, 1474, 1548, 1777, 2891, 3209, 3219, 3231, 3241 *A*, *B*, *C* = 7.420 33, 1.936 63, 1.585 13
11, C_5H_4CHO ($\tilde{X}$, ^{2}A′)	−306.271 12		138, 198, 285, 390, 506, 537, 604, 727, 738, 817, 858, 896, 913, 981, 1013, 1027, 1085, 1191, 1254, 1306, 1387, 1405, 1468, 1578, 1752, 2881, 3209, 3220, 3227, 3242 *A*, *B*, *C* = 7.903 21, 1.991 71, 1.590 80
$C_5H_4CHO + H$	−306.770 93	4.6	
	reaction 12 C_6H_6O (benzene oxide) $\rightarrow$ TS12 $\rightarrow C_6H_6O$ (oxepin)		
TS12 (^{3}A′)	−306.751 12	17.1	807i, 149, 323, 405, 429, 516, 543, 614, 667, 695, 745, 858, 907, 918, 932, 949, 1002, 1065, 1134, 1187, 1239, 1289, 1356, 1387, 1423, 1502, 1525, 3077, 3139, 3154, 3170, 3177, 3180 *A*, *B*, *C* = 4.428 10, 3.492 73, 2.155 71
12, oxepin (ã, ^{3}A′)	−306.818 41	−25.1	209, 229, 400, 452, 478, 521, 624, 656, 708, 777, 806, 910, 911, 913, 916, 950, 986, 1170, 1183, 1279, 1369, 1409, 1453, 1456, 1512, 1519, 1635, 3152, 3154, 3169, 3184, 3220, 3226 *A*, *B*, *C* = 3.908 89, 3.653 11, 1.888 34
	reaction 13 C_6H_6O (2,4−cyclohexadienone) $\rightarrow$ TS13 $\rightarrow C_6H_6O$ (*n*−butadienylketene)		
TS 13	−306.790 84	−7.8	225i, 118, 244, 268, 328, 395, 492, 531, 619, 709, 796, 815, 858, 902, 924, 942, 975, 1051, 1122, 1205, 1269, 1383, 1429, 1467, 1500, 1551, 1873, 3129, 3136, 3147, 3154, 3172, 3239 *A*, *B*, *C* = 4.287 601, 2.417 610, 1.675 447
13, *n*-butadienylketene (ã, ^{3}A′)	−306.79621	−12.4	29, 115, 163, 259, 317, 359, 435, 459, 544, 631, 675, 690, 794, 808, 888, 995, 1007, 1048, 1127, 1174, 1234, 1372, 1385, 1430, 1444, 1515, 2185, 3095, 3135, 3147, 3149, 3162, 3241 *A*, *B*, *C* = 4.088 71, 1.853 93, 1.513 18

[a] CBS-QB3 energies containing ZPE (scaling factor for frequencies is 0.99). [b] Energies containing ZPE relative to reactants. [c] Vibrational frequencies and rotational constants are determined at the B3LYP/6−311 g(d,p) level. [d] Approximate energy from PES calculations. Actual transition states could not be found (see text). Energies are from B3LYP/6-311G(d,p).

by −8.8 kcal mol^{-1} and has a barrier of approximately 4.9 kcal mol^{-1}. The chemically activated adduct can react on the triplet surface to form a number of products. The two lowest barriers are formation of phenoxy radical (−3.4 kcal mol^{-1} relative to reactants) and to formylcyclopentadiene (−1.8 kcal mol^{-1} relative to reactants). Collisional stabilization of the formylcyclopentadiene can occur, or the chemically activated aldehyde can go through an elimination reaction to form a cyclopentadienyl and formyl radicals. Using the results from Table 3, we can calculate Transition State Theory rate constants for the

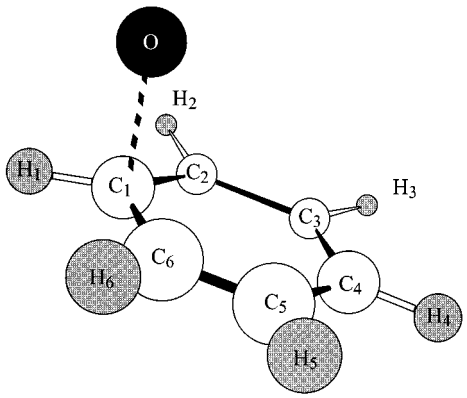

Figure 2. Atom labels for this study.

reactions shown in Figure 1 (Table 5) using the following estimate for the preexponential *A* factor

$$A = \frac{kT}{h}\left(\frac{1}{RT}\right)^{\Delta n} \exp(1 - \Delta n) \exp\left(\frac{\Delta S^{\ddagger}}{R}\right) \qquad (9)$$

where Δn is the change in the number of molecules in going from the reactants to the TS and $\Delta S^{\ddagger}$ is the change in entropy. Entropies are calculated using the harmonic oscillator (scaling factor = 0.97) and rigid rotor approximations with molecular parameters taken from B3LYP calculations. Activation energies are taken from CBS-QB3 calculations. We have used these Arrhenius parameters to estimate the rate constants for reactions at 298 and 1800 K, and these values are shown in Table 3. As these TST calculations predict, the most important high-pressure exit channel for the adduct on the triplet surface is the formation of phenoxy radical, **2**, followed by formylcyclopentadiene, **3**, and benzene oxide, **5**.

Formation of Adduct (Reaction 1). The initial step in this reaction is the addition of oxygen atom onto the aromatic ring. Because the ground state of O is ^{3}P, one would expect spin conservation to dictate that the product of this reaction is a triplet adduct. Our calculations on the triplet surface predict that the enthalpy of the triplet adduct is 8.7 kcal mol^{-1} lower in energy than the reactants in good agreement with the bond energy estimation shown above. Our calculations indicate that the singlet state of the adduct is higher in energy than the triplet though the exact amount was difficult to determine because of spin contamination problems. More extensive multireference calculations are needed to obtain accurate estimates of this splitting. As can be seen by the estimated rate constants in Table 5, the lifetime of the adduct at combustion temperatures is so small that intersystem crossing to the singlet potential energy surface may be minor.

Our calculations show that the potential energy barrier for this reaction step has the largest effect upon the overall activation energy for O(^{3}P) + C_6H_6. In Table 2, we make a comparison of the calculated barrier height for this step using different computational techniques. As can be seen, CBS-QB3 provides the most reasonable barrier energy (4.9 kcal mol^{-1}), and the density functional techniques all predict a barrier that is 3−4 kcal mol^{-1} too low. As mentioned above, this result is typical for B3LYP.[36−49]

The scheme below shows the molecular orbital structure for this step of the reaction. The reactants, transition state and adduct are all of C_s symmetry. Allowing the reaction to occur without symmetry produced no difference in the results. The transition state and adduct are both A″ with the singly occupied p-orbital of the oxygen atom parallel to the benzene ring.

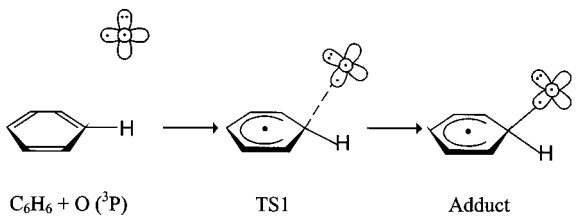

One can see from the calculated bond lengths shown in Table 4 that in TS 1, the C_2-C_3 bond length is nearly that of a double

TABLE 4: Selected Bond Lengths and Angles for Transition States at B3LYP/6-311G(d,p)

molecule	bond length (Å)		angles (degrees)	
Benzene[a]	C−H	1.0842		
	C−C	1.3933		
TS1	C_1−O	1.8842	O−C_1−C_4	100.5
	C_1−C_2	1.4289	H_1−C_1−C_4	164.7
	C_2−C_3	1.3182		
	C_3−C_4	1.4008		
TS2	C_1−O	1.2898	O−C_1−C_4	164.8
	C_1−C_2	1.4643	H_1−C_1−C_4	105.7
	C_2−C_3	1.3709		
	C_3−C_4	1.4102		
	C_1−H_1	1.6467		
TS3	C_1−O	1.2632	O−C_1−C_2	122.6
	C_1−C_2	1.5530	C_1−C_5−C_9	100.9
	C_2−C_3	1.4979	C_1−C_5−H_{10}	145.0
	C_3−C_4	1.4031		
	C_4−C_5	1.3783		
	C_5−C_6	1.4876		
	C_6−C_1	1.7822		
	C_6−C_2	1.4788		
TS4	C_1−O	1.4155	O−C_1−C_4	134.34
	C_1−H_1	1.3102		
	O−H_1	1.4155		
	C_1−C_2	1.4872		
	C_2−C_3	1.3606		
	C_3−C_4	1.4246		
TS5	C_1-O	1.4167		
	C_6-O	1.6903		
	C_1-C_2	1.4843		
	C_2-C_3	1.4303		
	C_3-C_4	1.3625		
	C_4-C_5	1.4636		
	C_5-C_6	1.4071		
	C_6-C_1	1.4741		
TS7	C_1-O	1.3190		
	C_1-H	1.7307		
	C_6-H	1.4766		
	C_1-C_2	1.3899		
	C_2-C_3	1.4003		
	C_3-C^4	1.4289		
	C_4-C_5	1.3877		
	C_5-C_6	1.4372		
	C_6-C_1	1.4840		
TS12	C_1-O	1.4110		
	C_6-O	1.4069		
	C_1-C_2	1.4715		
	C_2-C_3	1.4149		
	C_3-C^4	1.3718		
	C_4-C_5	1.4644		
	C_5-C_6	1.3774		
	C_6-C_1	1.8439		

[a] Experimental values for benzene r(C−C) = 1.084 Å, r(C−H) = 1.397 Å.[67]

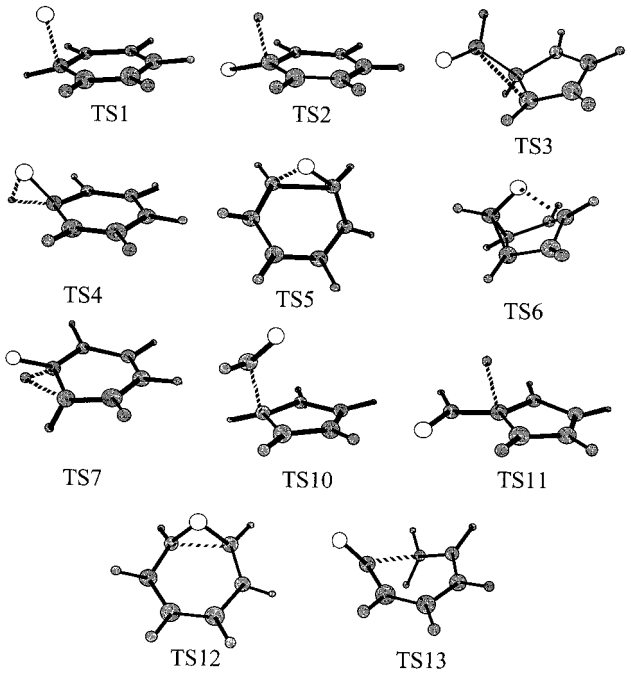

Figure 3. Calculated structures of the important transition states using B3LYP/6−311 g(d,p).

carbon−carbon bond suggesting that of the possible resonance structures shown below, R1 is the dominant structure.

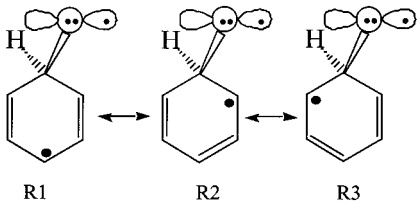

Formation of phenoxy radical (Reaction 2). This step leads to the formation of a ground-state phenoxy radical and hydrogen atom. Because of the high stability of the phenoxy radical, this step is calculated to be 6.3 kcal mol^{-1} exothermic and the calculated energy barrier is 5.3 kcal mol^{-1}. Our calculated overall standard enthalpy for the formation of phenoxy radical and hydrogen atom from C_6H_6 + O(^{3}P) ($\Delta_{react}H^{298}$) is −16.4 kcal mol^{-1} which compares well with the available experimental value of −14.3 kcal mol^{-1}.[57] The reverse reaction of H atom with phenoxy radical to form the adduct, **1**, has a calculated barrier of 11.7 kcal mol^{-1}. The rate for this reaction has not been measured but our calculated barrier is higher than the measured activation energy for the addition of H atom to benzene (4 kcal mol^{-1}).[58]

A schematic diagram of the important orbitals for this reaction are shown below. Phenoxy radical is formed by dissociation of the C_1-H_1 bond in the adduct and a rotation of the oxygen atom p-orbital so that the singly occupied orbital is perpendicular to the phenyl ring allowing for delocalization of the radical into

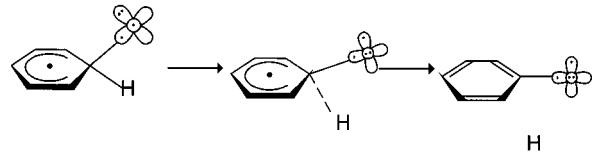

the aromatic ring. That is, there is a shift from an A″ (C_{2v} symmetry group) in the adduct to A′ in the transition state and product.

One would expect this reaction to have a late transition state with a resulting high preexponential factor. As Table 4 shows, the C_1-H_1 bond length is long (1.6467 Å) and the $O-C_1-C_4$ angle is large (164.8°), suggesting that the transition state is similar to the products. This results in a (low) preexponential factor because the ring vibrational modes are relatively high due to deolcalization of the unpaired electron.

Formation of formylcyclopentadiene and subsequent reactions (Reactions 3, 10, and 11). The reaction of the triplet adduct to form triplet formylcyclopentadiene, **3**, is slightly exothermic (−3.9 kcal mol^{-1}) and has a 6.9 kcal mol^{-1} barrier. TS 3 is highly strained due to the existence of three- and five-membered rings. As a result, the preexponential factor for this reaction is relatively low (Table 5). The TST rate constant for this channel from the adduct is significantly smaller at all temperatures than reaction 2 as is the RRKM rate constant. This is largely due to the difference in activation energy between these two channels. However, this difference in energy (1.6 kcal mol^{-1}) is within the uncertainty of the CBS technique being used. Thus, it is possible that reaction 3 could play a more important role in the title reaction than our predictions indicate.

The triplet state (ã, ^{3}A′) of **3** is a formed from the singlet ground state (X̃, ^{1}A′) by promoting an electron from a nonbonding p-orbital on the oxygen atom to a π^*-orbital on the ring as seen below. Further reaction to form cyclopentadienyl radical and HCO must be accompanied by a transition of a π electron from the ring back to the nonbonding orbital on the O atom. For this reason, there is a slight barrier (8.4 kcal mol^{-1}) to the reverse of reaction 10 and TS10 relative to **3** has an energy (14.4 kcal mol^{-1}) greater than the bond dissociation energy of **3** (6.0 kcal mol^{-1}). The standard enthalpy of formation of C_5H_5 + HCO is calculated to be −7.9 kcal mol^{-1} relative to the reactants compared with and experimental value of −11.5 kcal mol^{-1}.[59] However, there is substantial reported uncertainty in this experimental value.

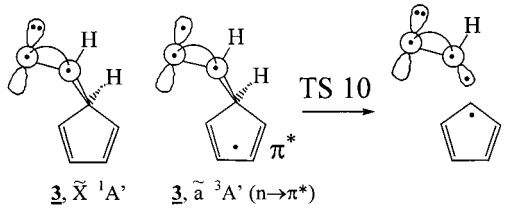

Formation of Phenol (Reaction 4). The reaction of the triplet adduct to form triplet phenol, though exothermic (−7.9 kcal mol^{-1}) has a high barrier (24.0 kcal mol^{-1}) typical of 1,2 hydrogen shifts[60] and similar to the barrier in reaction 7. Our CBS calculations can be calibrated by comparing the calculated enthalpy of formation of singlet phenol relative to the reactants to the experimental measurements. Our calculated standard enthalpy of reaction is −103.5 kcal mol^{-1} and the experimental value is −102.4 kcal mol^{-1}.[61] In addition, our calculated singlet−triplet splitting in this molecule, 84.2 kcal mol^{-1}, agrees with the experimental value of 81.6 kcal mol^{-1}.[62] Surprisingly, the preexponential factor is high for this reaction (Table 5), due to low frequency vibrational modes in the ring. This is because the transition state is early with much adduct character (Table 5).

As an aside, because singlet phenol is the lowest singlet product from this reaction, if a transition to the singlet surface were to occur it is likely that this species would be formed.

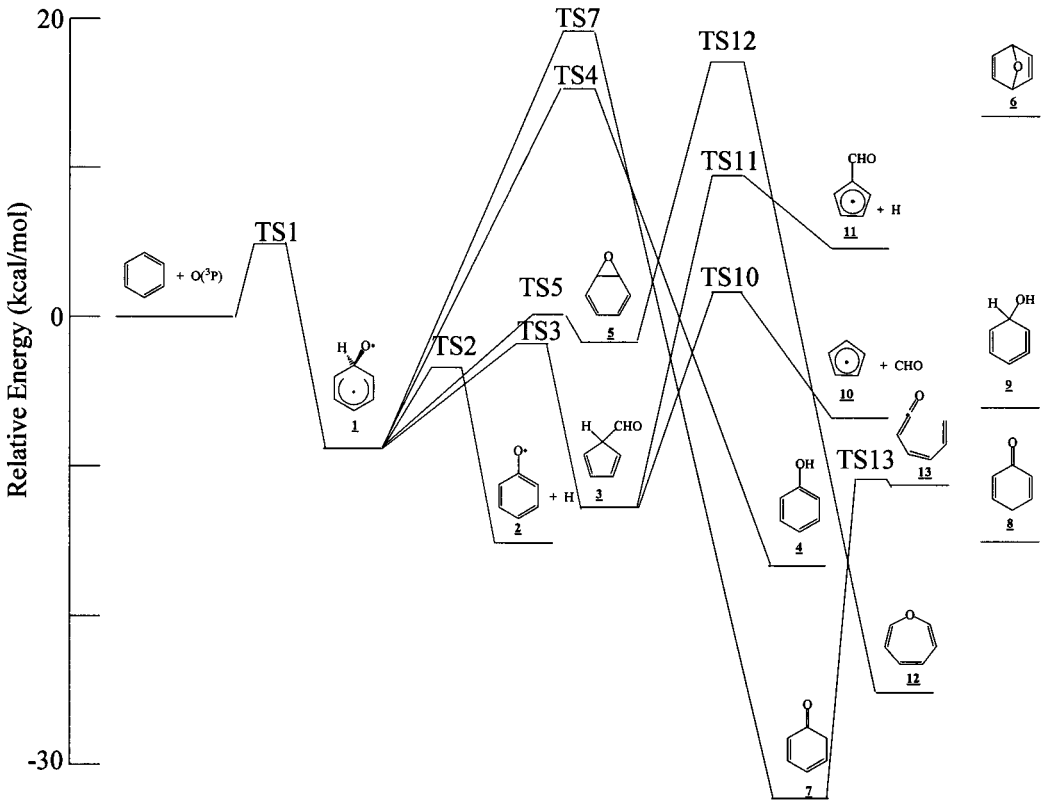

Figure 4. Illustration of the potential energy of triplet products and transition states in the benzene and oxygen atom reaction. The transition states for products ***6***, ***8***, and ***9*** are off the scale of the graph (see Table 3).

TABLE 5: Transisition State Theory High Pressure Limit Calculations of Rate Constants

			in units of cm^3 mol s		
reaction	ΔE^{298} TS kcal mol^{-1}[a]	ΔS^{298} TS cal mol^{-1}[b]	A^{298} [c]	k^{298} [d]	k^{1800} [d]
1 forward	4.3	−21.7	2.04×10^{13}	1.44×10^{10}	6.14×10^{12}
1 reverse	13.7	−1.0	1.01×10^{13}	8.43×10^{2}	2.17×10^{11}
2 forward	5.3	−2.2	5.47×10^{12}	7.27×10^{8}	1.25×10^{12}
3 forward	6.9	−2.3	5.39×10^{12}	4.53×10^{7}	7.79×10^{11}
3 reverse	10.1	−7.3	4.31×10^{11}	1.67×10^{4}	2.56×10^{10}
4 forward	24.2	−0.7	1.22×10^{13}	2.11×10^{-5}	1.39×10^{10}
5 forward	8.9	−2.5	4.84×10^{12}	1.45×10^{6}	4.03×10^{11}
5 reverse	1.6	−1.6	7.38×10^{12}	4.77×10^{11}	4.69×10^{12}
6 forward	33.7	−5.7	9.60×10^{11}	1.85×10^{-13}	7.7×10^{7}
7 forward	28.0	−1.8	6.68×10^{12}	1.92×10^{-8}	2.65×10^{9}
7 reverse	51.0	−4.5	1.76×10^{12}	6.47×10^{-26}	1.12×10^{6}
10 forward	14.2	−2.0	6.08×10^{12}	2.43×10^{2}	1.15×10^{11}
11forward	21.9	−3.8	2.45×10^{12}	2.02×10^{-4}	5.33×10^{9}
12 forward	18.6	−1.1	9.75×10^{12}	2.28×10^{-1}	5.40×10^{10}
13 forward	24.4	−1.2	9.24×10^{12}	1.26×10^{-5}	1.02×10^{10}

[a] Energy difference between reactants and transition state (including ZPE) from CBS-QB3 calculations. [b] Entropy difference between reactants and transition state, from B3LYP/6−311 g(d,p) calculations. [c] Arrhenius preexponential factor determined by eq 9. [d] Rate constants determined using ΔE as Arrhenius activation energy.

The high level of chemical activation (−102.4 kcal mol^{-1}) would be enough to overcome the barrier to form phenoxy radical (88.9 kcal mol^{-1})[63] and one might expect that phenoxy radical formation would dominate the singlet surface.

Formation of Benzene Oxide and Oxepin (Reactions 5 and 12). The formation of benzene oxide, **5**, from the adduct is exothermic (7.1 kcal mol^{-1}) with a 8.9 kcal mol^{-1} barrier. The transition state for this step is also tight, leading to a low preexponential factor. As a result, this channel does not play a significant role in the title reaction. We did not find a direct route for the formation of oxepin, **13** from the adduct **1**, although it can be formed in the triplet state from the benzene oxide, reaction 12. This step is exothermic (−23.4 kcal mol^{-1}) with a large barrier (18.6 kcal mol^{-1}). The photochemistry of benzene oxide and oxepin has been well studied in solution[64] and the gas phase[65] Reactions with triplet sensitizers show that **1** can be formed from triplet benzene oxide which is consistent with our reaction barrier of 1.9 kcal mol^{-1} for this reaction. Triplet sensitized photochemsitry of benzene oxide also showed the formation of phenol. This could be due to photochemistry of the adduct or hydrogen atom abstraction by phenoxy radical. However, because TS5 is significantly higher in energy than TS2 and TS3, these reactions are unlikely to play an important role in combustion chemistry.

Formation of bicyclo[2,2,1]hepta-7-oxa-2,5-diene (Reaction 6). Our CBS calculations suggest that this reaction step is highly

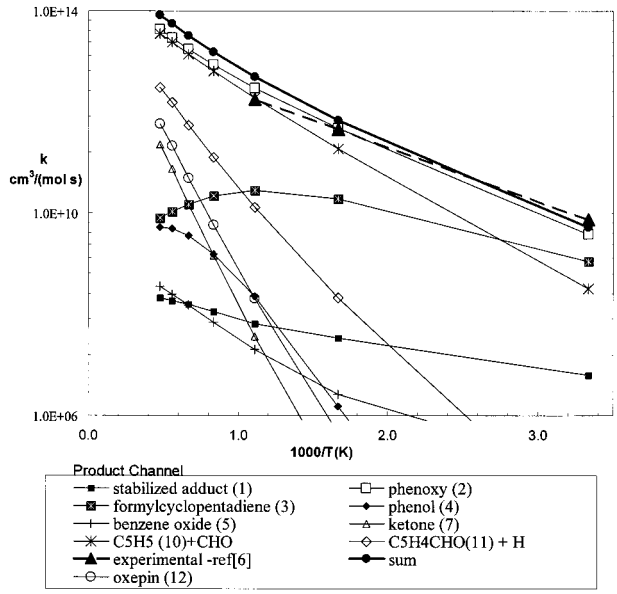

Figure 5. Calculated RRKM rate constants for formation of products from the reaction of oxygen atom (^{3}P) with benzene. Experimental data[6] (O + C_6H_6 _ Products) along with the sum of all reaction channels is plotted at a pressure of 100 Torr nitrogen.

endothermic, 22.2 kcal mol^{-1}. Furthermore, the reaction barrier is high, 34.2 kcal mol^{-1}, and the preexponential is low. As a result, it is unlikely that this pathway will be an important exit channel for the chemically activated adduct.

Formation of 2,4-cyclohexadienone and n-butadienylketene (Reactions 7 and 13). The reaction of the adduct to form 2,4-cyclohexadienone **7** is calculated to be exothermic (−32.2 kcal mol^{-1}), but because this reaction step is a 1,2 hydrogen shift, the barrier is high (28.0 kcal mol^{-1}). Because of its high reaction barrier, this reaction pathway does not contribute significantly in combustion. The further reaction of triplet 2,4-cyclohexadienone to yield triplet *n*-butadienylketene, **13**, is endothermic 21.0 kcal mol^{-1}, with a calculated barrier of 24.4 kcal mol^{-1}. The photochemical formation of *n*-butadienylketene from 2,4-cyclohexadienone as been reported in the literature,[64] but it is not clear if this reaction is on the triplet surface.

Formation of 2,5-cyclohexadienone and 2,4,5-cyclohexatrienol (Reactions 8 and 9). Reaction 8 is exothermic (−6.3 kcal mol^{-1}) but the high apparent reaction barrier (36.7 kcal mol^{-1}) make this reaction unlikely. Similarly, though Reaction 9 is only slightly endothermic (2.7 kcal mol^{-1}), the apparent (62.8 kcal mol^{-1}) barrier prevents this channel from contributing significantly. The long distances that the reactive hydrogens must travel in these reactions likely accounts for the high barriers.

Figure 5 displays the rate constants obtained from an RRKM modeling of the title reaction at 100 Torr, the pressure of the experimental values from ref 6. The dominant product channel at higher temperatures is phenoxy plus hydrogen atom, followed closely by the elimination reaction leading to the formyl and cyclopentadienyl radicals. Formation of the stabilized formylcyclopentadiene **3** is high at lower temperatures, but as temperature increases the collisional deactivation of an excited formylcyclopentadiene molecule is less likely. The experimental values found by Nicovitch[6] are in close agreement with our theoretical prediction.

Discussion

The computational results shown above present a picture that is qualitatively and quantitatively consistent with the data generated experimentally, although there are some differences in energetics which can probably be attributed to uncertainties in the molecular modeling process. However, the *interpretation* of the data presented by this work is somewhat different than that which is present in the literature. Of the experimental studies, only the study of Sibener et al.[5] directly observed the masses of reaction products although no study could analyze the molecular structure of the products. Sibener et al. concluded that the two primary channels for the title reaction were phenol and phenoxy + H with a minor channel being CO + cyclopentadiene. Our results suggest that the elimination of hydrogen directly from the triplet adduct has low barrier and is the dominant reaction at higher temperatures. Another route for hydrogen elimination does exist by first isomerizing the ring structure into formylcyclopentadiene and eliminating the tertiary hydrogen on the ring. Not only is this bond the weakest C−H bond of the molecule, but the products are stabilized by the resonance in the cyclopentadienyl system. The resulting barrier of this elimination step is 9.5 kcal mol^{-1} relative to stable benzene and oxygen.

Sibener et al. assigned the addition product to phenol, however the flame data of Bittner and Howard[66] indicate that a direct route to phenol is not possible. This work shows, instead, that the addition product is likely to be formylcyclopentadiene. The formylcyclopentadiene will be formed with a large amount of internal energy, so an elimination to form cyclopentadienyl and formyl radical is likely, especially at higher temperatures, when collisional stabilization occurs less frequently.

The observation of Sibener et al. that a minor C_5H_6 + CO channel existed was based on an analysis of the angle and velocity of the scattered mass 65 signal. An alternate interpretation of the crossed molecular beam data, and more likely from our results, is that a formyl radical was produced from a chemically activated formylcyclopentadiene molecule. Thus, all the results of the molecular beam study are consistent, in a qualitative sense, with the computational work presented here. The relative distributions of the three channels cannot be directly compared with the Sibener et al. result because the molecular beams do not have thermal energy distributions.

Conclusion

Major discrepancies between benzene flame data and elementary reaction modeling have led us to theoretically analyze the reaction pathways of the reaction C6H6 + O (3P) using ab initio methods at the B3LYP/cc-pVDZ and CBS-QB3 level of theory. Rate constants were found from RRKM theory using the vibration frequencies and energies calculated by Gaussian 98. The overall rate constant is in close agreement to overall rate constants in the literature. The major pathway contributions at combustion temperatures are the elimination of hydrogen to form a phenoxy radical, and the formation of the cyclopentadiene and formyl radicals. Our original hypothesis that the production rate of phenoxy in our modeling of the Bittner and Howard data is too high is not supported in the present work. That is, using the rate constants derived from this study still leads to a large over-prediction in the phenoxy profile of a benzene flame. Barring errors in the current calculations, we are forced to conclude that the second hypothesis, the destruction rates and/or the destruction channels for phenoxy are in error, is correct. However, it must be noted that the uncertainty in the CBS-QB3 method is approximately 2.8 kcal mol-1. If the

relative energy levels of TS2 and TS3 shifted by amounts within the error limits, the relative importance of the phenoxy and cyclopentadienyl channels would shift dramatically. Clearly, additional work is needed on phenoxy destruction channels in order test our second hypothesis.

Acknowledgment. We are very grateful to the National Science Foundation for our funding under Grant No. CTS-9215795, the NSF National Young Investigator Program, The Biomass Power Program of the Department of Energy (M.R.N.) and the National Center for Supercomputer Applications (NCSA). Grant No. CHE980028N

References and Notes

(1) Sawyer, R. F. *Twenty-Fourth Symposium (International) on Combustion*; The Combustion Institute, Pittsburgh, 1992; pp 1423−1432.

(2) Longwell, J. P. *Nineteenth Symposium (International) on Combustion*; The Combustion Institute, Pittsburgh, 1982; pp 1339−1350.

(3) Zhang, H.-Y.; McKinnon, J. T. *Combust. Sci. Tech.* **1995**, *107*, 261−300.

(4) Boocock, G.; Cvetanovic, R. J. *Can. J. Chem.* **1961**, *39*, 2436−2443.

(5) Sibener, S. J.; Buss, R. J.; Casavecchia, P.; Hirooka, T.; Lee, Y. T. *J. Chem. Phys.* **1980**, *72*, 4341−4349.

(6) Nicovich, J. M.; Gump, C. A.; Ravishankara, A. R. *J. Phys. Chem.* **1982**, *86*, 1684−1690.

(7) Ko, T.; Adusei, G. Y.; Fontijn, A. *J. Phys. Chem.* **1991**, *95*, 8745−8748.

(8) Gaffney, J. S.; Atkinson, R.; Pitts, J. N., Jr. *J. Am. Chem. Soc.* **1976**, *98*, 1828−1832.

(9) Sloane, T. M. *J. Chem. Phys.* **1977**, *67*, 2267−2274.

(10) Barry, N. J.; Fletcher, I. W.; Whitehead, J. C. *J. Phys. Chem.* **1986**, *90*, 4911−4912.

(11) Urena, A. G.; Hoffmann, S. M. A.; Smith, D. J.; Grice, R. *J. Chem. Soc., Faraday Trans. 2* **1986**, *82*, 1537−1541.

(12) Leidreiter, H. I.; Wagner, H. Gg. *Z. Phys. Chem. Neue Folge,* **1989**, *165*, 1−7.

(13) Tappe, M.; Schliephake, V.; Wagner, H. Gg. *Z. Phys. Chem. Neue Folge*, **1989**, *162*, 129−145.

(14) Lindstedt, R. P.; Skevis, G. *Combust. Flame* **1994**, *99*, 551−561.

(15) Chevalier, C.; Warnatz, J. *Fuel Chemistry Division, American Chemical Society*; 1991, *36*, 1486-1493.

(16) Bittker, D. A. *Combust. Sci. Tech.* **1991**, *79*, 49−72.

(17) Emdee, J. L.; Brezinsky, K.; Glassman, I. *J. Phys. Chem.* **1992**, *96*, 2151−2161.

(18) Mallard, W. G.; Westley, F.; Herron, J. T.; Hampson, R. F.; Frizzell, D. H. *NIST Chemical Kinetics Database-Ver. 5.0*; NIST Standard Reference Data, Gaithersburg, MD, 1993.

(19) Nicovich, J. M.; Ravishankara, A. R. *J. Phys. Chem.* **1984**, *88*, 2534.

(20) The dissociation energy of a π-bond can be estimated from the hydrogenation energy of a double bond, the C−H bond energy and the bond energy of H_2. $D°(C{=}C \rightarrow C{-}C) = \Delta_{hydrogenation}H + D°(C{-}H) - D°(H{-}H)$. For instance, for *cis*-2-butene, $\Delta_{hydrogenation}H = -28.3$ kcal/mol,[68] $D°(C{-}H) = 94.5$ kcal/mol,[69] and $D°(H{-}H) = 104.2$ kcal/mol[69] and $D°(C{=}C \rightarrow C{-}C) = 57.6$ kcal/mol.

(21) The aromatic resonance stabilization energy for benzene can be estimated as the difference between the enthalpy of hydrogenation of three triple bonds (−85.9 kcal/mol)[70] and the enthalpy of hydrogenation of benzene (49.06 kcal/mol).[71]

(22) The bond dissociation energy in dimethyl either is 82 kcal/mol,[69] for instance.

(23) The stabilization energy of the 2,4-cyclohexadienyl radical can be estimated by the difference between the enthalpy of hydrogenation of two double bonds (−56.6 kcal/mol[68]) and the actual enthalpy of the reaction of two moles of molecular hydrogen with 2,4-cyclohexadienyl radical to give cyclohexyl radical. The enthalpy of this reaction can be determined from the enthalpy of formation of 2,4-cyclohexadienyl radical (50 kcal/mol[69]) and the enthalpy of formation of cyclohexyl racical (13 kcal/mol[69]), −37 kcal/mol.

(24) Hehre, W. J.; Radom, L.; Schleyer, P. V. R.; Pople, J. A. *Ab Initio Molecular Orbital Theory*; Wiley: New York, 1986.

(25) Marcus, R. A. *J Phys Chem.* **1965**, *43*, 2658.

(26) Frisch, M. J.; Trucks, G. W.; Schlegel, H. B.; Gill, P. M. W.; Johnson, B. G.; Robb, M. A.; Cheeseman, J. R.; Keith, T.; Petersson, G. A.; Montgomery, J. A.; Raghavachari, K.; Al-Laham, M. A.; Zakrzewski, V. G.; Ortiz, J. V.; Foresman, J. B.; Peng, C. Y.; Ayala, P. Y.; Chen, W.; Wong, M. W.; Andres, J. L.; Replogle, E. S.; Gomperts, R.; Martin, R. L.; Fox, D. J.; Binkley, J. S.; Defrees, D. J.; Baker, J.; Stewart, J. P.; Head-Gordon, M.; Gonzalez, C., and Pople, J. A.; Gaussian 94, Revision B.3, Gaussian, Inc., Pittsburgh, PA, 1995.

(27) Turro, N. J. *Modern Molecular Photochemistry*; University Science Books: Sausalito, CA, 1991.

(28) Becke, A. D. *Phys. Rev. B* **1988**, *38*, 3098. Lee, C.; Yang, W.; Parr, R. G. *Phys. Rev. B* **1988**, *37*, 785.

(29) Dunning, T. H., Jr. *J. Chem. Phys.* **1989**, *90*, 1007.

(30) Foresman, J. B.; Frisch, A. E. *Exploring Chemistry with Electronic Structure Methods*, 2nd ed.; Gaussian, Inc: Pittsburgh, 1993. Foresman, J. B.; Frisch, A. E..; Ochterski, J. W.; Frisch, M. J., in preparation.

(31) Friderichsen, A. V.; Radziszewski, J. G.; Nimlos, M. R.; Winter, P. R.; Dayton, D. C.; David, D. E.; Ellison, G. B. *J. Am. Chem. Soc.*, in press 2000.

(32) Friderichsen, A. V.; Shin, E.-J.; Evans, R. J.; Nimlos, M. R.; Dayton, D. C.; Ellison, G. B. *Fuel*, submitted 2000.

(33) Radziszewski, J. G.; Nimlos, M. R.; Winter, P. R.; Ellision, G. B. *J. Am. Chem. Soc.* **1996**, *118*, 7400−7401.

(34) Petersson, E. J.; Nimlos, M. R.; Fanuele, J.; Lemal, D. M.; Ellison, G. B.; J. George Radziszewski *J. Am. Chem. Soc* **1997**, *119*, 11 122.

(35) Winter, P. R.; Rowland, B.; Hess, W. P.; Radziszewski, J. G.; Nimlos, M. R.; Ellison, G. B. *J. Phys. Chem.* **1998**, *102*, 3238.

(36) Mabel, A. M.; Lin, M. C.; Yu, T.; Morokuma, K. *J. Phys. Chem.* **1997**, *101*, 3189.

(37) Baker, J.; Muir, M.; Andzelm, J. *J. Chem. Phys.* **1995**, *102*, 2063.

(38) Stanton, R. V.; Merz, K. M., Jr. *J. Chem. Phys.* **1994**, *100*, 434.

(39) Deng, L.; Ziegler, T. *Int. J. Quantum Chem.* **1994**, *52*, 731.

(40) Baker, J.; Andzelm, J.; Muir, M.; Taylor, P. R. *Chem. Phys. Lett.* **1995**, *237*, 53.

(41) Durant, J. L. *Chem. Phys. Lett.* **1996**, *256*, 595.

(42) Sosa, C. P.; Lee, C. *J. Chem. Phys.* **1993**, *98*, 8004.

(43) Carpenter, J. E.; Sosa, C. P. *J. Mol. Struct. (THEOCHEM)* **1994**, *311*, 325.

(44) Barone, V.; Orlandini, L. *Chem. Phys. Lett.* **1995**, *246*, 45.

(45) Nachtigall, P.; Jordan, K. D.; Smith, A.; Jonsson, H. *J. Chem. Phys.* **1996**, *104*, 148.

(46) Oie, T.; Topol, I. A.; Burt, S. K. *J. Phys. Chem.* **1995**, *99*, 905.

(47) Dobbs, K. D.; Dixon, D. A. *J. Phys. Chem.* **1994**, *98*, 12584.

(48) Bach, R. D.; Glukhovstev, M. N.; Gonzalez, C.; Marquez, M.; Estevez, C. M.; Baboul, A. G.; Schlegel, H. B. *J. Phys. Chem. A* **1997**, *101*, 6092.

(49) Basch, H.; Hoz, S. *J. Phys. Chem. A* **1997**, *101*, 4416.

(50) Montgomery, J. A., Jr.; Frisch, M. J.; Ochterski, J. W.; Petersson, G. A. *J. Chem. Phys.* **1999**, *110*, 2822.

(51) Peng, C.; Schlegel, H. B. *Israel, J. Chem.*, **1993**, *33*, 449.

(52) Holbrook, K. A.; Pilling, M. J.; Robertson S. H. *Unimolecular Reactions* 2nd ed.; John Wiley and Sons: New York, 1996.

(53) Stein, S. E.; Rabinovitch, B. S. *J. Chem. Phys.*, **1973**, *58*(*6*), 2438.

(54) Gilbert, R. G. *Chem. Phys. Lett.* **1983**, *96*, 259.

(55) Gilbert, R. S.; Smith, S. C. *Theory of Unimolecular and Recombination Reactions*, Blackwell Scientific Publications: Cambridge, MA, 1990.

(56) Wang, H., Ph.D. Thesis, Pennsylvania State University 1992.

(57) This standard enthalpy of reaction can be calculated using the following values $\Delta fH0$ (benzene) = 19.82 ± 0.12 kcal/mol,[72] $\Delta fH0$ (O [3P]) = 59.555 ± 0.024 kcal/mol,[73] $\Delta fH0$ (phenoxy radical) = 13. ± 1. kcal/mol,[74] $\Delta fH0$ (H) = 52.1028 ± 0.0014 kcal/mol.[73]

(58) Baulch, D. L.; Cobos, C. J.; Cox, R. A.; Esser, C.; Frank, P.; Just, Th.; Kerr, J. A.; Pilling, M. J.; Troe, J.; Walker, R. W.; Warnatz, J. J. *Phys. Chem. Ref. Data* **1992**, *21*, 411.

(59) This standard enthalpy of reaction is calculated using the following experimental values in addition to those in ref 71: $\Delta fH0$ (C5H5) = 57.9 ± 1.5 kcal/mol,[76] $\Delta fH0$ (HCO) = 10. ± 1..[74]

(60) Batt, L.; Burrows, J. P.; Robinson, G. N. *Chem. Phys. Lett.* **1981**, *78*, 467.

(61) Using the values in ref 59 and $\Delta_f H°$ (phenol) = −23.03 ± 0.14[77]

(62) McClure, D. S. *J. Chem. Phys.*, **1949**, *17*, 905.

(63) Lovell, A. B.; Brezinsky, K.; Glassman, I. *Int. J. Chem. Kinet.* **1989**, *21*, 547.

(64) Jerina, D. M.; Witkop, B.; McIntosh, C. L.; Chapman, O. L. *J. Am. Chem. Soc.* **1974**, *96*, 5578.

(65) Klotz, B.; Barnes, I.; Becker, K. H.; Golding, B. T. *J. Chem. Soc., Faraday Trans.* **1997**, *93*, 1507.

(66) Bittner, J. D.; Howard, J. B. "Structure of Sooting Flames" In *Soot in Combustion Systems and its Toxic Properties*; Lahaye, J., Prado, G., Eds.; Plenum Press: New York, 1983.

(67) Herzberg, G. *Molecular Spectra and Molecular Structure III. Electronic Spectra and Electronic Structure of Polyatomic Molecules*; D. Van Nostrand Co.: Princeton, NJ., 1967.

(68) Kistiakowsky, G. B.; Ruhoff, J. R.; Smith, H. A.; Vaughan, W. E. *J. Am. Chem. Soc.* **1935**, *57*, 876.

(69) Benson, S. W. *Thermochemical Kinetics*, 2nd ed.; John Wiley and Sons: New York, 1976.

(70) Molnar, A.; Rachford, R.; Smith, G. V.; Liu, R. *Appl. Catal*., 9: 219 (1984).

(71) Kistiakowsky, G. B.; Ruhoff, J. R.; Smith, H. A.; Vaughan, W. E. *J. Am. Chem. Soc*. **1935**, *57*, 876.

(72) Prosen, E. J.; Gilmont, R.; Rossini, F. D. *J. Res. NBS* **1945**, *34*, 65.

(73) Cox, J. D.; Wagman, D. D.; Medvedev, V. A. *CODATA Key Values for Thermodynamics*; Hemisphere Publishing Corp.: New York, 1984.

(74) Tsang, W. *Energetics of Organic Free Radicals*; Martinho Simoes, J. A., Greenberg, A., Liebman, J. F., Eds.; Blackie Academic and Professional: London, 1996; p 22.

(75) Baulch, D. L.; Cobos, C. J.; Cox, R. A.; Esser, C.; Frank, P.; Just, Th.; Kerr, J. A.; Pilling, M. J.; Troe, J.; Walker, R. W.; Warnatz, J. J. *Phys. Chem. Ref. Data* **1992**, *21*, 411.

(76) McMillen, D. F.; Golden, D. M. *Annu. Rev. Phys. Chem.* **1982**, *33*, 493.

(77) Cox, J. D. *Pure Appl. Chem*. **1961**, *2*, 125.